

Electrochemical Sensing System for Detection of Organophosphate Neurotoxins

by

Alina Chanysheva

A thesis submitted to the Graduate Faculty of
Auburn University
in partial fulfillment of the
requirements for the Degree of
Master of Science

Auburn, Alabama
May 7, 2016

Keywords: tricresyl phosphate, alkaline hydrolysis, p-cresol,
electrochemical analysis, ultrasonic irradiation

Copyright 2016 by Alina Chanysheva

Approved by

Aleksandr Simonian, Chair, Alumni Professor of Materials Engineering
Dong-Joo Kim, Alumni Professor of Materials Engineering
Majid Beidaghi, Assistant Professor of Materials Engineering

Abstract

Jet engine oils contain appreciable amount of toxic ingredients, however are considered safe provided the oil stays in the engine and appropriate precautionary measures are taken. Organophosphorus compound tricresyl phosphate (TCP), known to be a neurotoxin, is widely used as an anti-wear additive in jet engine oils. Bleed air system for cabin air delivery implies a risk of exposing passengers of airliners to TCP and products of its hydrolysis. The development of a highly-sensitive, robust, time and cost-efficient device for TCP detection on an airliner is of an increased practical interest. Electrochemical detection method was chosen in this work as it proved to be the most efficient tool for TCP detection. Non-electroactive TCP was hydrolyzed, and products of alkaline hydrolysis were detected via electrochemical methods.

In flight conditions, it is critical to have a reaction design that would ensure a safe, robust and cost-effective hydrolysis of TCP with a high reaction conversion, thus requiring a reliable and effective reaction enhancement method. Ultrasonic irradiation is employed as a novel approach to enhance the alkaline hydrolysis reaction. TCP is hydrolyzed very slowly in neutral or acidic media, and considerably faster in alkaline solution. Boiling-enhanced alkaline TCP hydrolysis was performed to demonstrate the effectiveness of ultrasound irradiation acceleration of this reaction.

An additional cresol detection technique, UV-vis spectrophotometry with the demonstrated limit of detection of p-cresol of 100 μM , was used for validation of the effectiveness of alkaline hydrolysis reaction. Electrochemical detection provided a significantly improved limit of p-cresol detection of 0.5 μM .

From the perspective of developing a portable and time-efficient sensor for use on airliners, ultrasonic irradiation and electrochemical techniques proved to be effective for enhancing alkaline hydrolysis of TCP and rapid and highly-sensitive detection of cresol.

Dedication

I dedicate this thesis to my parents, Liliya Chanysheva and Nail Chanyshiev, and my sister Lolita. Thank you for inspiring me to pursue all of my dreams.

Acknowledgments

First and foremost, I would like to express my sincere gratitude to my advisor, Dr. Aleksandr Simonian for all his tremendous support, and encouragement. Without his continuous optimism, enthusiasm and patience this thesis would not have been possible. His guidance into the world of sensors and electrochemistry has been vital during my graduate studies. I will always be grateful for an opportunity to work in his research group and to learn from him.

I would like to thank my committee members, Dr. Kim and Dr. Beidaghi for their participation in my thesis committee.

I would also like to thank Dr. Mary Arugula, postdoctoral fellow in our lab, for providing advice and expertise in experimental and theoretical aspects of scientific research and for many hours of lab training. I thank my lab members, Yuanyuan Zhang, Fuling Yang, and Lang Zhou for a friendly atmosphere in the lab. I want to thank Steven Moore for his help with instruments and equipment. I would also like to thank all of my fellow graduate students in Materials Engineering, and all of my friends in Auburn for making my time here so enjoyable.

I am truly thankful to my best friends, with the warmest hearts imaginable, Darya Kandratsenia and Yulya Lefterova Coste for their emotional support and continuous encouragement from a distance.

Finally and most importantly, I would like to express my deepest gratitude to my parents, Liliya and Nail Chanshev, my sister Lolita, my grandmothers Mariyam and Alzira, my aunts Alfiya and Razida, my cousins Rafael and Timur. My parents have made my graduate studies possible, words cannot express how grateful I am for their love and support. Being engineers, they continuously provided invaluable advice throughout this project. I thank them for believing in me.

Table of Contents

Abstract.....	ii
Dedication.....	iv
Acknowledgments.....	v
List of Tables	x
List of Figures	xi
List of Abbreviations	xiii
Chapter 1: Research Motivation and Objectives	1
1.1 Thesis Organization	2
Chapter 2: Introduction and Literature Review	3
2.1 Sensors	3
2.1.1 Chemical Sensors.....	3
2.1.2 Electrochemical Sensors	4
2.1.2.1 Potentiometry.....	5
2.1.2.2 Amperometry / Voltammetry.....	6
2.2 Tricresyl Phosphate.....	7
2.3 TCP Contamination of Cabin Air in an Aircraft.....	9
2.4 Ultrasonic Irradiation	11
Chapter 3: Materials and Methods.....	15
3.1 Reagents and Solutions	15

3.2 Instrumentation and Equipment.....	16
3.2.1 Potentiostat.....	16
3.2.2 Working Electrodes	16
3.2.3 Auxiliary and Reference Electrodes	17
3.2.4 Flowcell for Amperometric Measurement.....	17
3.2.5 Ultrasonic Processor	19
3.2.6 Coil-Reflux Condenser	19
3.2.7 UV-VIS Spectrophotometer.....	19
3.3 Experimental Procedures	20
3.3.1 Overview of Experimental Procedures	20
3.3.2 Preparation of pTCP and Sodium Hydroxide Solutions	20
3.3.3 Experimental Set-up for Ultrasonic Irradiation-Enhanced pTCP Hydrolysis	21
3.3.4 Experimental Set-up for Boiling-Enhanced pTCP Hydrolysis	22
3.3.5 Cyclic Voltammetry in a Batch Mode	22
3.3.6 Amperometry in a Flow Mode.....	23
3.3.7 Spectrophotometric Measurements.....	23
Chapter 4: Results and Discussions	25
4.1 Electrochemical Response of Cresols.....	25
4.2 Electrochemical Detection of P-cresol. Calibration Curve.....	26
4.3 Spectrophotometric Detection of P-cresol. Calibration Curve	27
4.4 Ultrasonic Irradiation-Enhanced pTCP Hydrolysis. Electrochemical Detection of Product	30
4.5 Spectrophotometric Detection of Product of Ultrasonic Irradiation – Enhanced pTCP Hydrolysis.....	32

4.6 Boiling - Enhanced pTCP Hydrolysis. Electrochemical Detection of Product	33
4.7 Spectrophotometric Detection of Product of Boiling - Enhanced pTCP Hydrolysis	34
Chapter 5: Overall Conclusions and Suggestions for Future Work.....	36
References	38

List of Tables

Table 1: TCP alkaline hydrolysis half-lives [53]	9
Table 2: Determination of p-cresol concentration in product of alkaline hydrolysis of pTCP enhanced by ultrasonic irradiation using the p-cresol calibration curve...	31
Table 3: Determination of p-cresol concentration in product of alkaline hydrolysis of pTCP enhanced by boiling using the p-cresol amperometric calibration curve..	34

List of Figures

Figure 1: Chemical structure of TCP and its main isomers [52]	7
Figure 2: Alkaline hydrolysis of TCP [34]	8
Figure 3: Schematic representation of air recirculation system in an airliner cabin [51] ..	10
Figure 4: Ultrasound cavitation bubble growth and implosion in a liquid irradiated with ultrasound [39].....	11
Figure 5: Three reaction zones in the cavitation process [46]	12
Figure 6: (a) Electrochemical Analyzer (Model: 160C, P/N: uEA160C10002); (b) CHI 760E electrochemical workstation.....	16
Figure 7: System for flow mode amperometric detection of cresol: A – dual syringe pump, B – 6-port valve with 50 μ l loop for loading liquid samples, C – electrochemical flowcell (auxiliary electrode block).....	18
Figure 8: Overall experimental procedure	20
Figure 9: Experimental set-up for ultrasonic irradiation-enhanced pTCP hydrolysis	21
Figure 10: Experimental set-up for boiling-enhanced pTCP hydrolysis	22
Figure 11: Cyclic voltammetry of 100 μ M p-cresol on a bare glassy carbon electrode in 0.1 M PBS buffer at pH 6.67 at scan rates of 10, 20, 50, 80, 100, 120, 150, 200 mV/s in the range of potential from 0 to 800 mV vs Ag/AgCl. The increase of the scan rates is indicated by the arrow direction.....	26
Figure 12: (a) Amperometry of pure p-cresol with concentrations in nM; (b) Calibration curve for p-cresol electrochemical detection. Concentrations of p-cresol are ranging from 500 nM to 4000 nM. Note: current of 0 nM injections was subtracted from all sample injections. The R^2 coefficient of the linear fit is 0.9963.....	27
Figure 13: (a) UV-Vis absorption spectra of p-cresol (concentration units are μ M). The absorbance peak at 525 nm indicates p-cresol. (b) Calibration curve of UV-Vis absorption spectra of p-cresol. The R^2 coefficient of the linear fit is 0.9747 ...	29

Figure 14: (a) Amperometry of products of pTCP alkaline hydrolysis reaction enhanced by ultrasonic irradiation (raw data). Concentrations shown in this amperometry curve are initial concentrations of pTCP, μM . (b) Linear plot of amperometry of pTCP alkaline hydrolysis reaction enhanced by ultrasonic irradiation. Note: in plotting (b), current of 0 μM injection was subtracted from all injections. The R^2 coefficient of the linear fit is 0.951931

Figure 15: UV-Vis absorption spectra of product of ultrasonic irradiation-enhanced pTCP hydrolysis. Concentrations are the pTCP concentrations32

Figure 16: (a) Amperometry of products of pTCP alkaline hydrolysis reaction enhanced by boiling (raw data). Concentrations shown in this amperometry curve are initial concentrations of pTCP, μM . (b) Linear plot of amperometry of pTCP alkaline hydrolysis reaction enhanced by boiling. Note: in plotting (b), current of 0 μM injection was subtracted from all injections. The R^2 coefficient of the linear fit is 0.990633

Figure 17: UV-Vis absorption spectra of product of boiling-enhanced pTCP hydrolysis. Concentrations are the pTCP concentrations. Limit of detection is 100 μM pTCP. The absorbance peak is observed at 525 nm, which allows to detect the product of hydrolysis, cresol.....35

List of Abbreviations

TCP	Tricresyl Phosphate
pTCP	P-tricresyl Phosphate
oTCP	O-tricresyl Phosphate
CV	Cyclic Voltammetry
LSV	Linear Sweep Voltammetry
ECS	Environment Control System
GC	Gas Chromatography
GC/MS	Gas Chromatography - Mass Spectrometry
TCL	Thin-layer Chromatography
HPLC	High-performance Liquid Chromatography
OPIDN	Organophosphorus-induced Delayed Neuropathy
GC/NPD	Gas Chromatography with Nitrogen-phosphorus Detector
GC/FPD	Gas Chromatography with Flame Photometric Detector
DI	De-ionized
PBS	Phosphate Buffer Saline
GC	Glassy Carbon

Chapter 1. Research Motivation and Objectives

Non-pesticidal triaryl organophosphates gained a significant research interest due to their neurotoxicity and reports of cabin air pollution on aircrafts. The development of rapid, simple, inexpensive TCP detection system for application in an airliner cabin is of significant interest. Gas chromatography with a nitrogen-phosphorus sensitive detector (GC/NPD), a flame photometric detector (GC/FPD) [28], a mass spectrometric (MS) recognition [29], high-performance liquid chromatography (HPLC) [30], thin layer chromatography (TLC) [31] are well-established laboratory techniques that can be employed for TCP detection [32, 33]. However, application of such techniques requires high-cost equipment, trained personnel, and time-consuming detection procedures. All these factors, and the limitations to miniaturization of a detection device, make these techniques impractical onboard. Electrochemical techniques, on the other hand, are a promising solution to the challenge of finding a time and cost-efficient detection method for TCP. Since electrochemical detection requires an electroactive compound, the non-electroactive TCP is converted to cresols via alkaline hydrolysis. Electroactive products of this reaction, cresols, are detected by amperometric techniques.

A sensing system for TCP electrochemical detection that employs a hydrolysis reaction conducted at an elevated temperature of 230 °C with complete evaporation of TCP and its pathway through a catalyst column, implying heterogeneous catalysis process, was previously reported by Yang et. al. [34-36]. The need for high temperatures and prolonged

time periods for reaction to occur define the challenging nature of hydrolysis of organophosphates [37].

The objectives of this research project are the development of an alternative approach to accelerating TCP hydrolysis and optimization of the electrochemical detection of reaction products. The reaction and detection steps would have a potential of integration into a portable sensor.

1.1 Thesis Organization

The current chapter provides the motivation for this research work. Chapter 2 presents the introduction and literature review, and is divided into sections that give information on chemical and electrochemical sensors, potentiometry, amperometry, tricresyl phosphate and contamination of cabin air in an aircraft, and ultrasonic irradiation phenomena. Experimental procedures are discussed in Chapter 3 which includes information on the reagents and solutions preparation, alkaline hydrolysis reaction process, and procedures for detection of cresol by amperometry and UV-Vis spectrophotometry. Chapter 4 provides the discussion of experimental results, which includes electrochemical and spectrophotometric calibration curves for pure p-cresol detection and the curves of detection of the product of hydrolysis reaction. Overall conclusions and suggestions for future work are presented in Chapter 5. All references are listed after Chapter 5.

Chapter 2. Introduction and Literature Review

2.1 Sensors

Technological advancements in engineering and science have led to the development of the multidisciplinary field of sensors. A device that detects changes in physical variables, which include temperature, pressure, humidity, mass, strain, voltage, is termed a sensor. Physical variables are converted into a universal signal via a transducer which is an important component of all sensors. There are several classes of sensors, based on the physical variable that is being detected [1].

Biosensors is an important class of sensors. The type and the concentration of a specific analyte are the variables of interest in biosensors. A sequence of nucleic acid (DNA, RNA), a bacterium, a protein, a biochemical compound are examples of analytes. Conventional sensors (temperature, humidity, pressure, mass, light transducers) cannot be used to determine the type and the concentration of an analyte. In order to fulfill this task there is a need for a bioreceptor, and biosensors come into play. Bioreceptor, a biological material, examples of which include antibodies, nucleic acids, enzymes, viruses, bacteria, is capable of specifically binding to a target analyte.

2.1.1 Chemical sensors

Chemical sensor contains a chemically selective layer, film, or membrane, and at its core it has a physical transducer, or reference electrode. This class of sensors provides

information on chemical nature of its environment. The main characteristics of a chemical sensor, sensitivity, selectivity, lifetime, response time, are controlled by the composition and the form of the chemically selective layer [2].

2.1.2 Electrochemical Sensors

Electrochemical sensors, a subclass of chemical sensors, are devices with working principle based on an induced chemical change leading to an electrical response. Their design uses an electrode as the transduction element [3]. Most of the electrochemical sensing techniques employ changes in potential and current. The categories of electrochemical sensors, distinguished based upon modes of signal transduction, are potentiometric, voltammetric and conductometric [4]. Potentiometric sensors are simple to use, and are characterized as having high selectivity and low cost, which makes them usable for field operations [5]. In contrast, voltammetric sensors are more sensitive and faster than potentiometric devices. Other groups of electrochemical sensors include chemiresistors and capacitive sensors, which rely on resistivity and impedance measurements, and devices that rely on conductivity changes of ions.

Nowadays, electrochemical sensors are widely used in environmental, clinical, industrial, agricultural analyses, as well as in every-day life, for instance, a conductometric oxygen partial pressure sensor in automobiles, blood glucose sensor, carbon monoxide detector with an electrochemical cell.

2.1.2.1 Potentiometry

An exchange of electrons between compound in a solution and a sensing element is the principal phenomenon in potentiometric sensors. Direct potentiometric measurements require an ion-selective electrode, which is an indicator electrode that selectively measures the activity of a chemical compound. The ion-selective electrodes are mostly nonporous membrane-based devices that have the filling ion solution of a constant activity inside. The membrane selectively binds ions and the potential is produced across the membrane. The resulting potential of ion-selective electrode relative to the potential of the reference electrode is dependent on the activity of the target ion in the solution of interest. The electrode potential, E , is defined by the Nernst equation [6] as

$$E = E_0 - 2.303 \frac{RT}{n_e F} \log_{10} (a_A + \beta_{AB} a_B), \quad (2.1)$$

where E_0 is an electrode material-dependent constant, R is the universal gas constant, T is the absolute temperature, n_e is the number of electrons involved in the reaction, F is the Faraday constant, a_A is the activity of species A, a_B is the activity of species B, β_{AB} is the selectivity coefficient of an A species-sensitive electrode to species B.

Concentration of species A, c_A , its activity, a_A , and activity coefficient, γ_A , are related to each other by

$$a_A = \gamma_A c_A \quad (2.2)$$

Ion-selective electrodes have a wide linear range and a fast response [3].

2.1.2.2 Amperometry / Voltammetry

Amperometric detection is based on the principle of the current production during oxidation or reduction of species at an electrode. The produced current is directly proportional to the concentration of the species. Chronoamperometry is a method that uses an electrode that has some initial rest potential at which molecules in the surrounding solution are not oxidized or reduced. The potential is suddenly changed and this initiates an electrochemical reaction. The step-wise change of the potential can cause an immediate and complete reaction in the analyzed substance, thus a concentration gradient is produced between the electrode surface and the surrounding solution and diffusion of the compound towards the electrode is initiated. The depletion of the solution next to the electrode occurs as the reaction continues, and the concentration gradient decreases, which causes the current decrease. The current-time relationship is defined by the Cottrell equation [7]

$$i_d = \frac{nFAD^{1/2}c}{\pi^{1/2}t^{1/2}}, \quad (2.3)$$

where i_d is the current, n is the number of electrons, F is the Faraday constant, A is the area of an electrode, D is the diffusion coefficient, c is the bulk concentration of the analyte, t is the time.

Linear sweep voltammetry (LSV) technique involves a regularly changing waveform applied to a working electrode. Cyclic voltammetry (CV), an analysis mode similar to the LSV, is often the first technique to apply at the inception of an electroanalytical study. It provides the information on the location of redox potentials of electroactive compounds and the influence of the media on the redox process. During the

potential sweep, current resulting from the applied potential is measured. The resulting cyclic voltammogram shows characteristic peaks caused by the formation of the diffusion layer at the electrode surface.

2.2 Tricresyl Phosphate

Tricresyl phosphate (TCP) is an organophosphorus compound widely used as an anti-wear additive in aircraft turbine engine oils, a component in flame retardants, plasticizers, and extraction solvents, due to being non-flammable and non-explosive. In jet engine oils, TCP concentrations are 2–3% [20, 21]. Commercial TCPs are mixtures of isomers (Figure 1), which include the most toxic isomer *o*-tricresyl phosphate (*o*TCP).

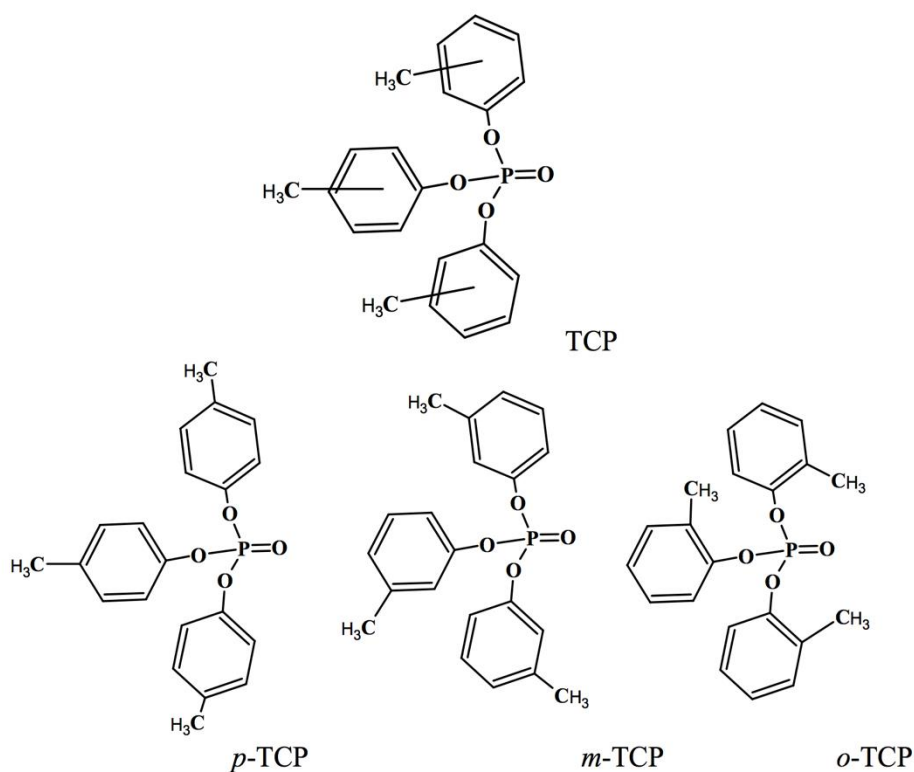


Figure 1: Chemical structure of TCP and its main isomers [52]

In neutral or acidic media TCP hydrolysis occurs very slowly, and in alkaline solution this reaction proceeds considerably faster. This reaction produces three molecules of cresol from one molecule of TCP. The reaction of alkaline hydrolysis of TCP is demonstrated in equation 1.4 and Figure 2 [34]. Table 1 shows hydrolysis half-lives in alkaline solution [53].

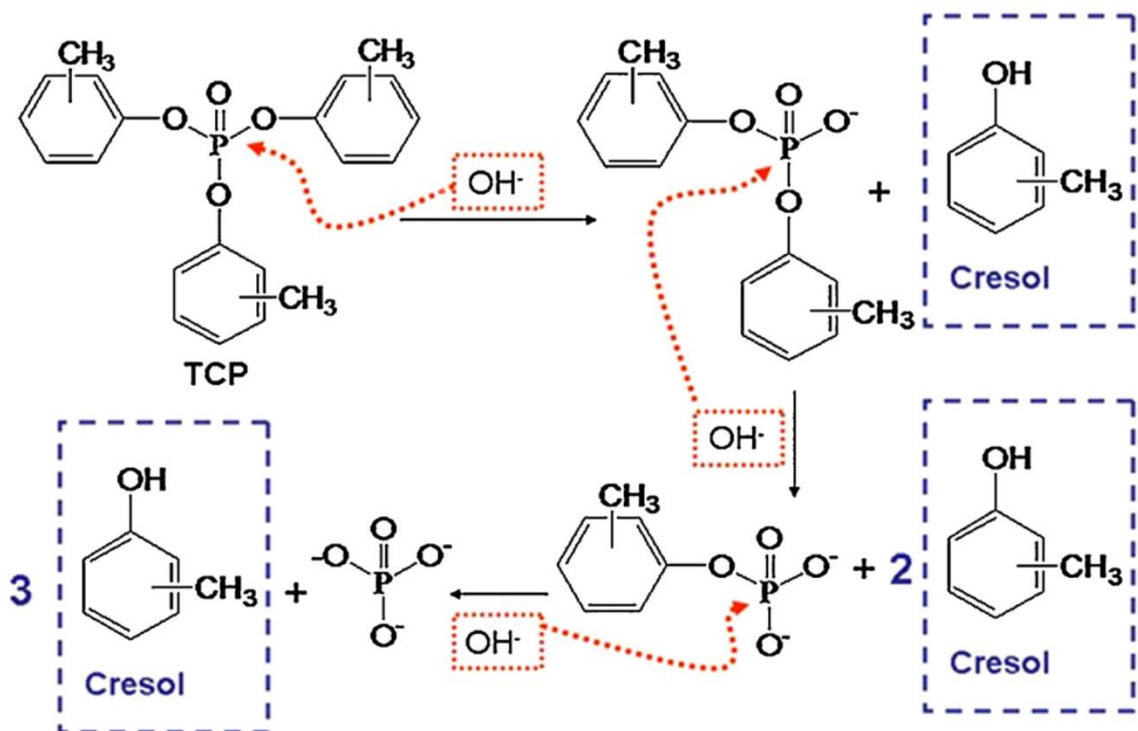


Figure 2: Alkaline hydrolysis of TCP [34]

Table 1: TCP alkaline hydrolysis half-lives [53]

Compound	Solution	Temperature (°C)	pH	Half-life
Tri-p-cresyl phosphate	0.2 N NaOH / acetone (1:1)	22	13	1.66 h
Tri-m-cresyl phosphate	0.1 N NaOH / acetone (1:1)	22	13	1.31 h

Gas chromatography (GC) is widely used for determining TCP. Other applicable analytical methods are GC-mass spectrometry (GC/MS), thin-layer chromatography (TLC) for edible oil analysis, high-performance liquid chromatography (HPLC), and colorimetry [54 – 57].

2.3 TCP Contamination of Cabin Air in an Aircraft

Organophosphates-based hydraulic fluids have been used in high-performance aircraft since the 1970s [8]. Over the past 30 years, there have been reports of illness of cabin crew and passengers associated with bleed-air incidents on commercial airliners [9-14]. At a cruising altitude of 11,000 m (37,000 ft) the ambient air temperature is -55°C (-67 F), the atmospheric pressure is about 30 kPa, and the moisture content is close to zero. Passengers and crew are protected from these extreme ambient conditions by an environment control system (ECS), which bleeds air from engine compression stages [15]. The most commonly used cabin air delivery method is mixing the bled air and the recirculated air [16]. Figure 3 shows air recirculation system in an airliner cabin. Air enters through the aircraft's jet engines, where it becomes compressed and hot, then it is directed

to the air conditioning units where it is cooled dramatically. Next, the outside air is combined with cleaned recirculated air to produce a 50/50 mix at the mixing manifold. Consequently, air is supplied into the cabin via overhead outlets. Eventually, used air is discharged to maintain the balance with the incoming outside air [51].

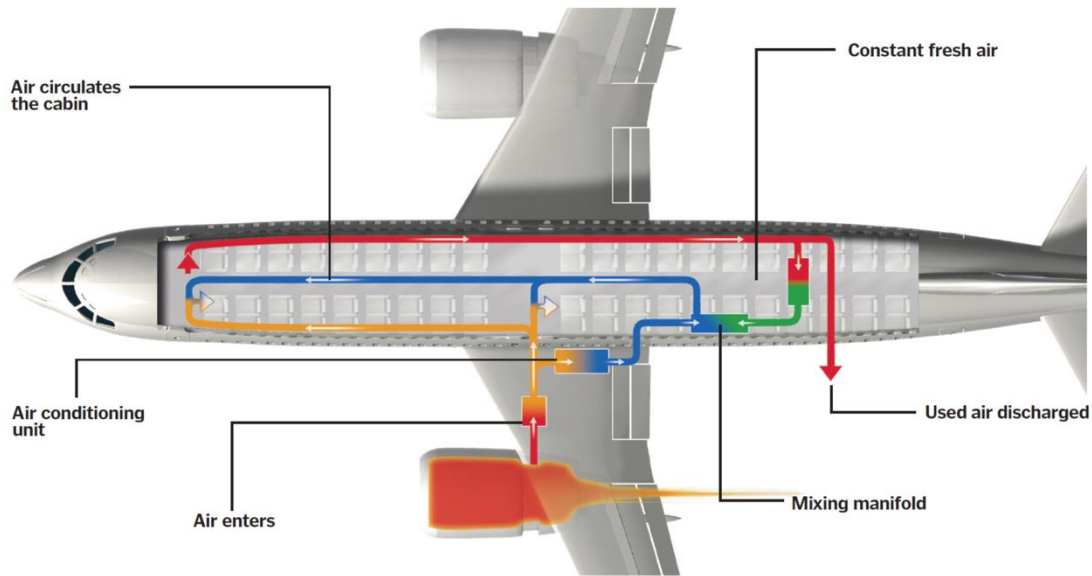


Figure 3: Schematic representation of air recirculation system in an airliner cabin [51]

As a result of leakage of engine-oil seals, jet engine oil fumes may contaminate the cabin air through the bleed air system. When engine lubricating oils and hydraulic fluids are at high temperatures around 525°C (engine conditions in some aircrafts), TCP isomers are released and trapped in air that is supplied to the cabin. It is not possible to control or eliminate contamination by increasing the ventilation flow rate [17]. Passengers and crew-members exposed to contaminated cabin air experience short or long-term symptoms which include dizziness, cognitive problems, disorientation, uncontrolled tremors [18, 19]. The adverse effect of TCP on a human body is explained by the fact that acetylcholine

esterase [22] and carboxyesterases [23], vital enzymes, are inhibited by this compound. Prolonged exposure to TCP may cause organophosphorus-induced delayed neuropathy (OPIDN) [24-27].

2.4 Ultrasonic Irradiation

Ultrasonic technology has been shown as an effective method for the destruction of pollutants, organic compounds, in the field of wastewater treatment [46]. The enhanced mass-transfer processes, thermolysis, shear degradation, chemical-free oxidation are the advantages of this technology. Ultrasonic irradiation is associated with cavitation phenomenon which includes the formation of cavitation bubbles, their growth, followed by their collapse, and a release of a large magnitude of energy (Figure 4) [39].

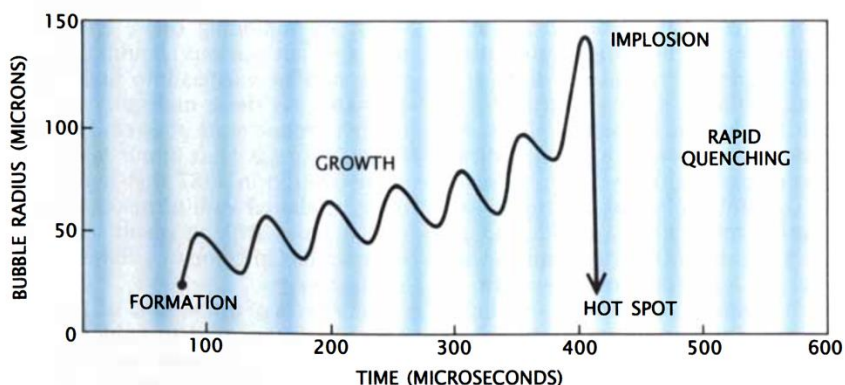


Figure 4: Ultrasound cavitation bubble growth and implosion in a liquid irradiated with ultrasound [39]

Free radicals produced during the cavitation bubbles collapse, and localized extreme conditions with enormous temperature up to 5000 K and pressure up to 1000 atm [44, 45] make the sonochemical process a promising method for enhancement of chemical

reactions. Sonochemical reactions are most-commonly explained using the hot-spot theory [46], which is based on the vision of microbubbles as small microreactors [53]. There are three zones in a cavitation bubble, according to the temperature profile studies (Figure 5) [46]. The core of the bubble is the thermolytic center (hot spot), which is characterized by the localized hot temperature around 5,000 K and high pressure around 500 atm during final collapse of cavitation. In aqueous solutions pyrolysis of bubble water molecules occurs inside this region with formation of hydroxyl and hydrogen radicals in the gas phase. The substrate reacts with the hydroxyl radical or pyrolysis occurs. Between the cavitation bubble and bulk liquid is the interfacial region, here, in aqueous phase, a reaction similar to hot spot occurs. In addition to that, hydroxyl-radical recombine forming hydrogen peroxide. In the third region, the bulk region, the reaction between the substrate and the hydroxyl-radical or hydrogen peroxide occur, and the temperature is around the room temperature.

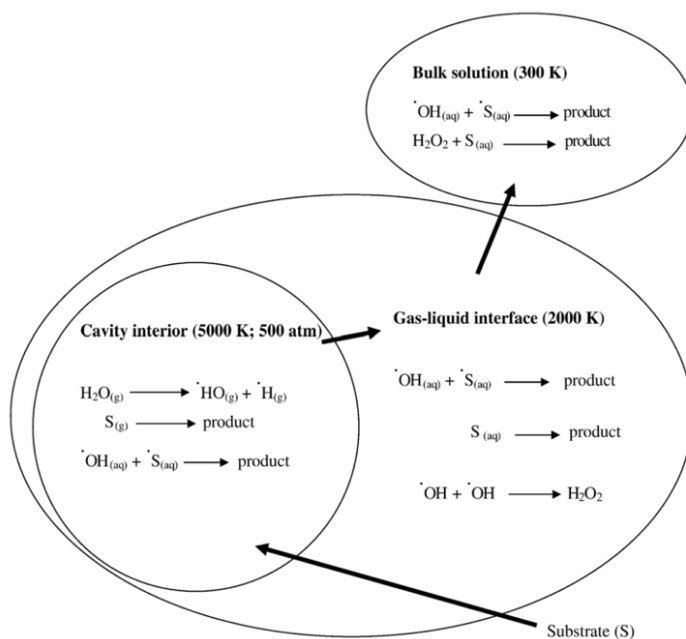


Figure 5: Three reaction zones in the cavitation process [46]

In homogeneous and heterogeneous media the effects of ultrasound are different. For the former, production of new chemical species occurs during cavitation and sonochemical reactions, and mechanical effects induced in liquid system enhance the reactions in the latter. [47].

Not only chemical effects are produced via ultrasound irradiation, physical effects (sonophysical) occur when liquid medium absorbs the acoustic energy from sound waves. Liquid medium starts flowing along the wave's propagation direction. Among the physical effects are microstreaming, microstreamers, microjets, and shock waves, where the fluid movement is turbulent, and cavitation bubbles create a microscale velocity gradient [48]. Ultrasound produces fluid movement which results in enhancement of mass-transfer processes between solid-bulk and gas-bulk interfaces. Therefore, mixing, breaking down of particles and macromolecules, extraction, and desorption processes are enhanced [49].

The phenomena of sonochemistry has been recognized for decades, however there is still no full understanding of the mechanisms of homogeneous and heterogeneous sonochemistry. Industrial scale applications of sonochemistry are in pollution control. The use of sonochemistry in organometallic synthesis, biphasic systems, catalytic reactions, and organic electrochemistry and the practical considerations for process optimization [41].

The cavitation collapse is strongly affected by the physicochemical properties of the solvent and the solute [42]. Solvents with high vapor pressure (VP), low surface tension (σ), and low viscosity (μ) are more prone to the formation of cavities. Bubble formation results from the breakage of the intermolecular forces in the liquid. Cavities are harder to

be formed in high density solvents with high surface tensions, and viscosities, however more extreme conditions in the bubbles exist in such solvents [43].

Chapter 3. Materials and Methods

3.1 Reagents and Solutions

Aqueous solutions were prepared with de-ionized (DI) water from the Milli-Q Direct system (resistivity 18.2 M Ω •cm). Phosphate buffer saline (0.1 M) (PBS) (pH=6.67) was prepared from sodium phosphate dibasic (Na₂HPO₄) (Sigma-Aldrich), potassium phosphate monobasic (KH₂PO₄) (Sigma-Aldrich), and sodium chloride (NaCl) (Fisher Scientific). Adjustment of the pH of the 0.1M PBS was performed by aqueous NaOH (Fisher Scientific). Ten mM stock solution of pure p-cresol (Sigma-Aldrich) was prepared in PBS. Ten mM stock solution of pure pTCP (MP Biomedicals) was prepared in methanol (99.8% purity) (BDH-VWR). The solution of 0.5 M NaOH (Fisher Scientific) was prepared in anhydrous denatured ethanol (Amresco Inc.). Acid diazo-reagent (dye) for spectrophotometric detection was prepared by dissolving 0.8 g of p-nitroaniline (Alfa Aesar) in DI water and adding 20ml of 20% hydrochloric acid to this mixture. To remove the residual slick, the solution was then decanted. The final step in preparation of the dye included addition of 50% sodium nitrite (NaNO₂) solution until the reagent was entirely colorless [40]. Buffer for spectrophotometric detection was prepared from NaHCO₃ (Sigma-Aldrich) and Na₂CO₃ (Sigma-Aldrich).

3.2 Instrumentation and Equipment

3.2.1 Potentiostat

All amperometric measurements were performed on Electrochemical Analyzer (Model: 160C, P/N: uEA160C10002, Homiangz LLC) (Figure 6a). The electrode leads coming out of the potentiostat are differentiated by color of the insulation on their alligator clips. The red lead corresponds to the working electrode, yellow and green leads are the reference and auxiliary electrodes respectively. Cyclic voltammetry studies were performed on CHI 760E electrochemical workstation (CH Instruments, Inc.) (Figure 6b).



(a)

(b)

Figure 6: (a) Electrochemical Analyzer (Model: 160C, P/N: uEA160C10002); (b) CHI 760E electrochemical workstation

3.2.2 Working Electrodes

Glassy carbon (GC) electrodes (BASiTM) were used as the working electrodes. The GC electrodes used for batch mode experiments were a 3 mm diameter GC rods embedded inside an insulating material of length 75 mm. For flow mode amperometry measurements, the working electrode block was a 2 mm diameter glassy carbon embedded inside an insulating material.

Preparation procedures for working electrodes prior to every voltammetric or amperometric experiments included consecutive polishing over 1, 0.3, and 0.05 μm α -alumina slurries (Buehler) along with rinsing with DI water between different slurries, polishing was followed by ultrasonic cleaning (Branson 1510) in ethanol for 10 minutes, and the preparation was completed by drying under nitrogen atmosphere. There was no modification of the GC electrodes performed.

3.2.3 Auxiliary and Reference Electrodes

A rod-shaped platinum wire of diameter 1 mm embedded inside an insulating material of length 75 mm was used as an auxiliary electrode (BASi™), and a silver-silver chloride (Ag/AgCl) with 3 M KCl internal solution (BASi™) was used as the reference electrode for cyclic voltammetry batch mode experiments. The auxiliary electrode and the reference electrode were rinsed thoroughly in DI water and dried before use. The storage solution for the reference electrode was the 3 M KCl solution. Cyclic voltammetry measurements were performed in a glass beaker with a plastic cap with holes for assembling electrodes.

3.2.4 Flowcell for Amperometric Measurement

The stainless steel electrochemical detection flowcell (auxiliary electrode block) (BASi™) model MF-1092 was used for flow mode amperometric experiments. The flowcell is the cross flow and includes a phenolic base, arms, and inlet/exit connections. The assembly was done by placing a thin-layer gasket over the pins of the flowcell, followed by placing the working electrode block over the gasket and attaching the backing

plate with the quick release mechanism over the working electrode block. The alignment pins on the flowcell insure the proper alignment of the thin-layer gasket and the working electrode. The Ag/AgCl reference electrode was inserted into the port on the top of the flowcell and fixed with the reference electrode retainer. The fluid flowing through the flow block was in continuous contact with all the three (working, auxiliary, and reference) electrodes.

The flow mode was established and maintained at 10 ml/hr by using a dual syringe pump (KD Scientific). A 6-port valve (Valco Instruments Co. Inc.) with a 50 μ l loop was used for loading liquid samples of pure p-cresol and hydrolysates. The system for amperometric detection in a flow mode, containing the pump, the 6-port valve, and the electrochemical detection flowcell, is shown in Figure 7.

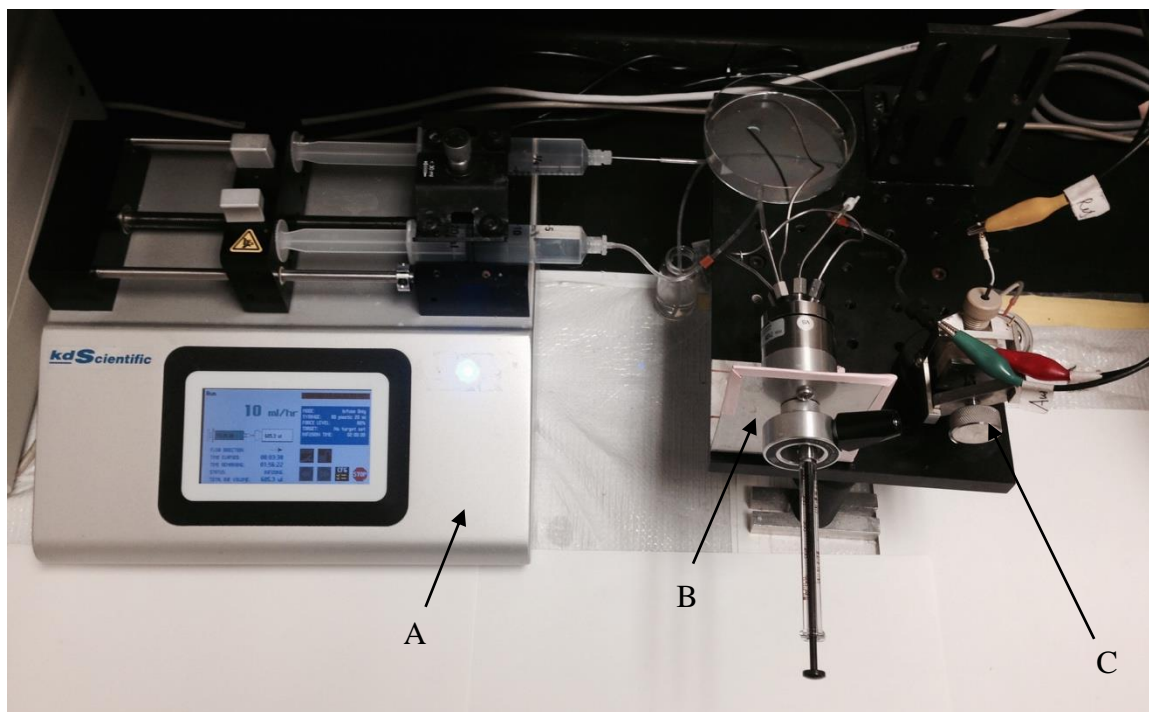


Figure 7: System for flow mode amperometric detection of cresol: A – dual syringe pump,

B – 6-port valve with 50 μ l loop for loading liquid samples, C – electrochemical flowcell (auxiliary electrode block)

3.2.5 Ultrasonic Processor

Ultrasonic irradiation during the TCP hydrolysis reaction was performed by ultrasonic processor Vibra-cell VC750 (Sonics & Materials Inc.) operating at 20 kHz and input power of 750 W. The process parameters were as follows: pulse 30/10, Amp 35%. The tip of the ultrasonic processor was rinsed with ethanol and DI water upon completion of irradiation process.

3.2.6 Coil-Reflux Condenser

Boiling-enhanced pTCP alkaline hydrolysis process involved the application of the coil-reflux condenser (Sial, Czechoslovakia), pear-shaped boiling flask (50ml) (Sial, Czechoslovakia), a magnetic stirrer with ceramic heating plate C-MAG HS 7 (IKA Works Inc.), and silicone oil (Sigma-Aldrich).

3.2.7 UV/VIS Spectrophotometer

Spectrophotometric detection of pure p-cresol, as well as the products of pTCP hydrolysis, cresols, was performed on the Ultrospec 2100 Pro UV/visible spectrophotometer (Biochrom Ltd.). SWIFT II applications software (Amersham Biosciences) was operated in the spectral scanning mode with the scan speed of 1800 nm/min for analysis of the absorption spectra of cresols of different concentrations.

3.3 Experimental Procedures

3.3.1 Overview of Experimental Procedures

Experimental procedures of this work are conveniently divided into two flows. First flow includes alkaline hydrolysis of pTCP conducted using ultrasonic irradiation for reaction enhancement. Consequently, detection of the products of reaction, cresols, is performed by two independent techniques: amperometry, and UV-vis spectrophotometry. Second flow uses boiling-enhanced alkaline hydrolysis of pTCP. Similarly, the detection of the products of reaction is performed by amperometry, and UV-vis spectrophotometry. A schematic of the overall experimental procedure is shown in Figure 8.

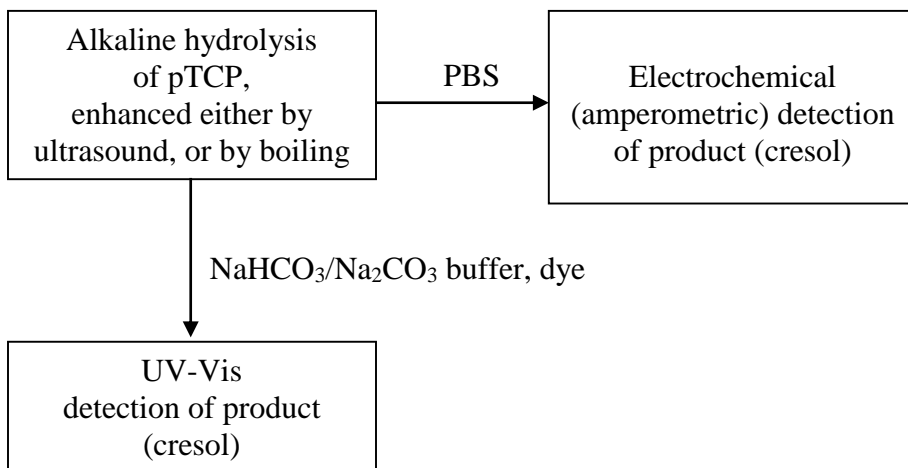


Figure 8: Overall experimental procedure

3.3.2 Preparation of pTCP and Sodium Hydroxide Solutions

A 10 mM stock solution of p-TCP in methanol was prepared for every experimental

procedure. The stock solution was consequently diluted to 1 mM, which was used directly in hydrolysis reactions. Sodium hydroxide solution (0.5 M) was prepared by dissolving the pellets in ethanol, and used as a reagent in a liquid phase. The stoichiometric amount of sodium hydroxide solution was added to the 1 mM p-TCP solution for each hydrolysis reaction.

3.3.3 Experimental Set-up for Ultrasonic Irradiation-Enhanced pTCP Hydrolysis

Immediately upon preparation the liquid mixture of pTCP and sodium hydroxide was subjected to ultrasonic irradiation performed in 8 runs for 8 min per run (pulse 30/10 Amp 35%), longer runs caused loss of products due to evaporation. Figure 9 depicts the ultrasonic irradiation process.

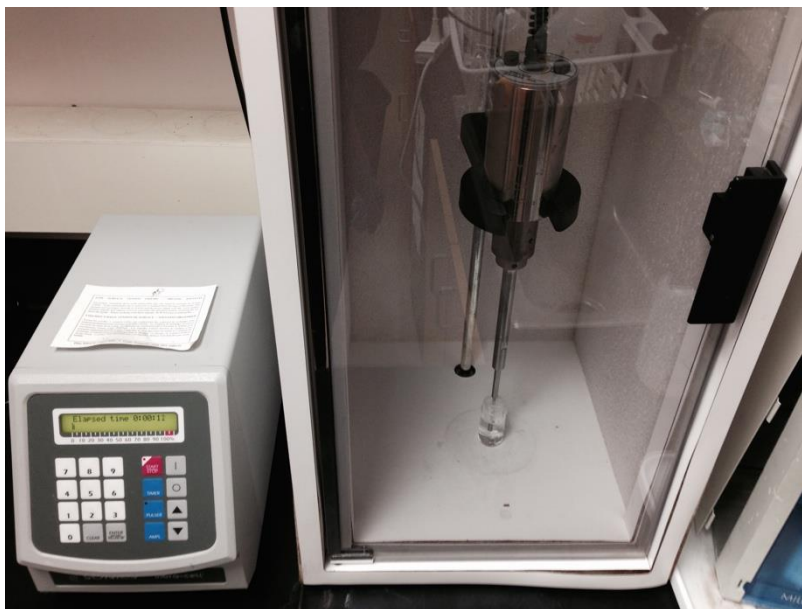


Figure 9: Experimental set-up for ultrasonic irradiation-enhanced pTCP hydrolysis

In between the ultrasonic runs the cooling periods, of 5 min each, were provided. Upon completion of the ultrasonic irradiation runs the liquid mixture of reagents and

products of hydrolysis was analyzed electrochemically, solutions of various concentrations were prepared in PBS for amperometric tests.

3.3.4 Experimental Set-up for Boiling-Enhanced pTCP Hydrolysis

Immediately upon preparation the mixture of solution of pTCP (1 mM) in methanol with stoichiometric amount of sodium hydroxide solution (0.5 M) in ethanol was subjected to boiling with coil-reflux condenser (Figure 10). The reacting mixture was confounded in a pear-shaped 50 ml boiling flask, and a coil-reflux condenser was assembled on its neck. Silicon oil, heated on a ceramic heating plate, provided the conditions for boiling the reacting mixture at temperature 85 °C, controlled by an external thermometer. Cooling water supply to the condenser was maintained during the boiling process.

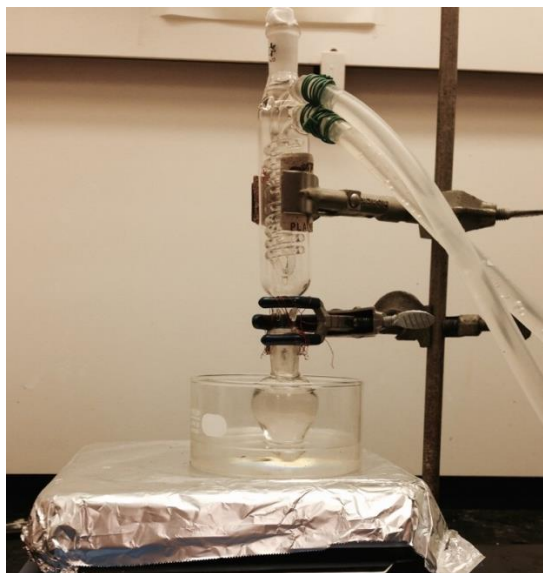


Figure 10: Experimental set-up for boiling-enhanced pTCP hydrolysis

3.3.5 Cyclic Voltammetry in a Batch Mode

Cyclic voltammetry was performed to determine the electrochemical activity of

cresols. A three-electrode cell was used in a batch mode in which glassy carbon, platinum, and Ag/AgCl (3 M KCl) served as the working, auxiliary and reference electrodes respectively. The glassy carbon working electrode was polished and subjected to ultrasonic cleaning before the experiment. Cyclic voltammetry was performed on a bare working electrode. The first cyclic voltammogram (CV) was taken in 5 ml of 0.1 M PBS, pH 6.67 between 0 mV and 800 mV vs. Ag/AgCl reference electrode. Consequently, 500 μ l of 1 mM p-cresol were added to the buffer solution such that the final concentration was 100 μ M, the potential was between 0 mV and 800 mV vs. Ag/AgCl. The scan rates were as follows: 10, 20, 50, 80, 100, 120, 150, 200 mV/s.

3.3.6 Amperometry in a Flow Mode

Pure p-cresol was analyzed using flow mode amperometry. A dual syringe pump operated at a flow mode of 10 ml/h maintained the flow mode during experiments. Upon establishing the PBS (0.1 M, pH=6.67) baseline, the following concentrations of p-cresol in PBS were injected through the 6-port sample valve: 500, 1000, 2000, 3000, and 4000 nM.

Product of pTCP alkaline hydrolysis was also analyzed via amperometry in a flow mode. Product was diluted by 0.1 M PBS (pH 6.67) down to 1 to 6 μ M solutions and injected into the flow system.

3.3.7 Spectrophotometric Measurements

UV-vis absorption spectra measurements for varying concentrations of p-cresol were performed using the acid diazo-reagent (dye) [40]. The wavelength range from 300

to 700 nm was chosen, the scan speed was 1800 nm/min. The measurement began with a reference of the 0.2 M sodium carbonate – bicarbonate buffer (pH 9.70). The reference cuvette measurement is followed by the next cuvette containing 10 μM p-cresol in the 0.2 M $\text{NaHCO}_3/\text{Na}_2\text{CO}_3$ (pH 9.70) solution and the dye. Using this technique, the UV-vis absorption spectra for the following concentrations of p-cresol were measured: 10, 20, 30, 40, 50, 60, 70, 80, 90, 100, 200, 300, 400, 500 μM .

Chapter 4. Results and Discussions

4.1 Electrochemical Response of Cresols

Cyclic voltammetry was performed to determine the electrochemical activity of cresols. The measurements in the three-electrode cell were conducted in a batch mode. Phosphate buffer saline (0.1 M, pH 6.67) was initially in the cell. Cyclic voltammogram of 100 μM p-cresol (Figure 11) performed from 0 V to 0.8 V vs Ag/AgCl at scan rates from 10 mV/s to 200 mV/s shows the response current of electroactive species. A quick increase in current at the beginning of each potential scan is observed due to the charging current, and is followed by a flat line. The onset of p-cresol oxidation is observed starting from around 0.6 V, which is indicated by the increase in current on a cyclic voltammetry curve, and produced a peak at around 0.72 V vs Ag/AgCl in the forward scan. No peak was observed in the reverse scan. The absence of a reduction peak suggests that p-cresol undergoes irreversible oxidation at around 0.72 V. With the increasing scan rate the whole i-V cycle expanded due to increased charging current, and the peak current increased. Cresol oxidation is a diffusion-controlled process [34], thus peak current on Figure 11 is proportional to the scan rate. The effect of scan rate on the peak current position is observed as slight shifting of the peaks positions.

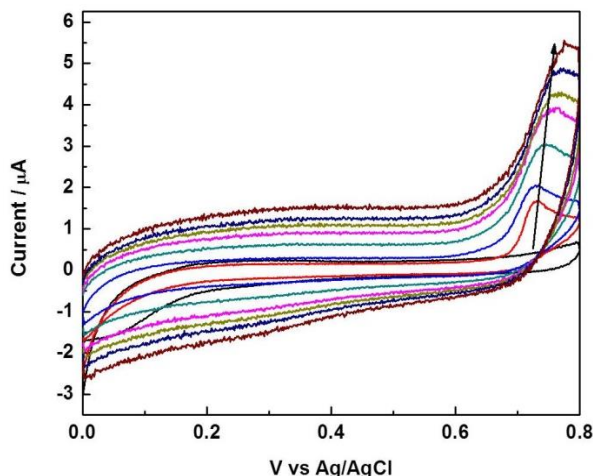


Figure 11: Cyclic voltammetry of 100 μM p-cresol on a bare glassy carbon electrode in 0.1 M PBS buffer at pH 6.67 at scan rates of 10, 20, 50, 80, 100, 120, 150, 200 mV/s in the range of potential from 0 to 800 mV vs Ag/AgCl. The increase of the scan rates is indicated by the arrow direction. The onset of p-cresol oxidation is observed starting from around 0.6 V, as indicated by the increase in current. The oxidation peak at 0.72 V vs Ag/AgCl is observed on this voltammogram in the forward scan.

4.2 Electrochemical Detection of P-cresol. Calibration Curve

Pure p-cresol solutions in 0.1 M PBS (pH 6.67) of various concentrations were tested for building a calibration curve of pure p-cresol. Amperometry with the potential of 0.72 V vs Ag/AgCl was conducted in a flow mode using a valve injection unit with a 50 μl sample injecting loop. A constant flow rate of 10 ml/hr was maintained by a syringe pump, five p-cresol samples of concentrations 500, 1000, 2000, 3000, 4000 nM were injected into the sample loop. The detection limit of p-cresol was determined as 500 nM, using the signal-to-noise ratio ($S/N=3$). Previously reported limit of p-cresol detection using electrochemical techniques was 600 nM [60]. The peak current increases linearly with p-

cresol concentrations. The R^2 coefficient of the linear fit is 0.996. The p-cresol calibration curve, shown on Figure 12, provides the reference for electrochemical detection of the products of pTCP hydrolysis. The amperometric current-concentration of the analyte relationship is linear, according to Cottrell equation (eq. 2.3).

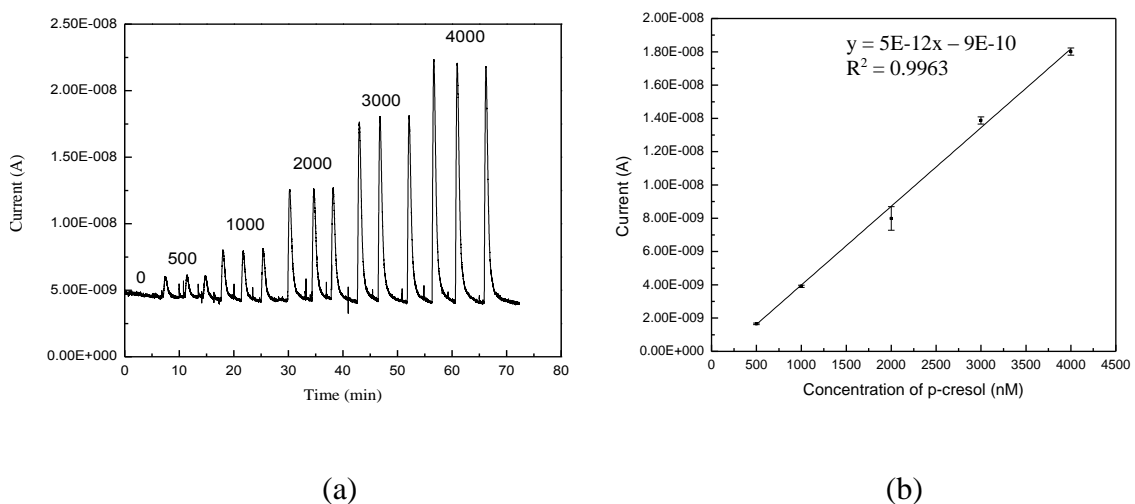


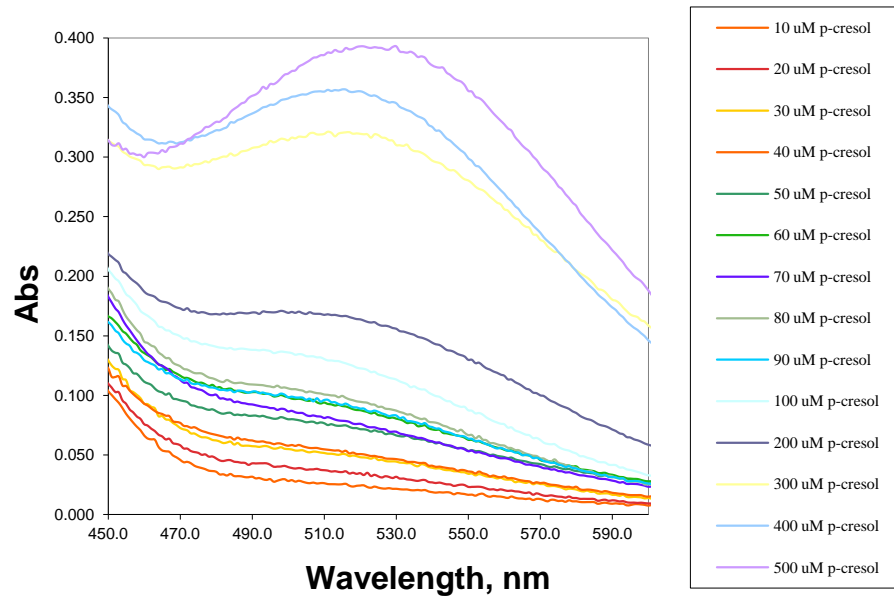
Figure 12: (a) Flow mode amperometry of pure p-cresol. Numbers over the peaks indicate the concentration of p-cresol (nM). (b) Calibration curve for p-cresol electrochemical detection (amperometry). Limit of detection is 500 nM. Each p-cresol concentration was injected 3 times and yielded 3 current peaks in each repetition of amperometry, data points on the calibration curve correspond to the average of 3 repetitions. Error bars are the standard deviation of the 3 repetitions. Note: current (signal) of 0 nM p-cresol injections was subtracted from all sample peak currents. The R^2 coefficient of the linear fit is 0.9963.

4.3 Spectrophotometric Detection of P-cresol. Calibration Curve

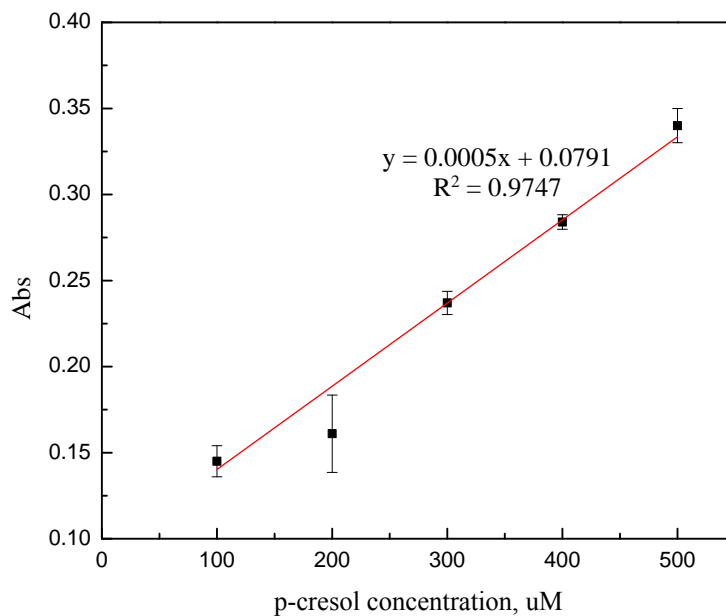
UV-vis absorption spectra measurements for various concentrations of p-cresol were performed, and calibration curve was obtained (Figure 13). The absorbance peak for

cresol isomers is located between 510 and 530 nm [58]. The peaks on Figure 13 indicate p-cresol. Varying concentration of p-cresol caused a slight shifting in the peak position which is acceptable for such concentration range of analyte [58].

The UV-vis spectra yield the limit of p-cresol detection of 100 μM using the signal-to-noise ratio ($S/N=3$). Lowering the concentration of p-cresol in the 0.2 M sodium carbonate – bicarbonate buffer ($\text{pH}=9.70$) down to the range from 10 to 90 μM resulted in no absorbance peaks. The p-cresol calibration curve provides the reference for spectrophotometrical detection of the products of pTCP hydrolysis. Electrochemical detection of p-cresol has a significantly improved detection limit compared to spectrophotometry, thus making amperometry a prospective technique for integration into a portable detection device. The significance of UV-vis spectra measurements in this work is in verification of pTCP hydrolysis destruction via detecting the product of reaction.



(a)



(b)

Figure 13: (a) UV-Vis absorption spectra of p-cresol (concentration units are μM). The absorbance peak between 510 and 530 nm indicates p-cresol. (b) Calibration curve of UV-Vis absorption spectra of p-cresol. Data points correspond to the average of 3 repetitions of UV-Vis

experiment. Error bars are the standard deviation of the 3 repetitions. The R^2 coefficient of the linear fit is 0.9747.

4.4 Ultrasonic Irradiation-Enhanced pTCP Hydrolysis. Electrochemical Detection of Product

Ultrasonic irradiation enhancement of chemical reactions is affected by the ultrasonic power. Higher reaction conversion can be achieved by using a higher power ultrasound [46]. Studies of phenolic compounds degradation show applications of power from 200 to 850 W, depending on the initial concentration of a compound [59]. Ultrasonic processor power of 750 W was used in this work. Product of ultrasonic irradiation enhanced pTCP alkaline hydrolysis, hydrolysate, was diluted with 0.1 M PBS (pH 6.67) down to concentrations from 1000 nM to 6000 nM in terms of initial pTCP concentrations. Amperometry of hydrolysate in a flow mode was performed for the detection of the product of alkaline hydrolysis of pTCP, p-cresol, and is shown on Figure 14. Control injection was the 0 nM pTCP. Unlike pTCP, cresol is electroactive, thus the amperometric test provides quantitative detection of p-cresol. Determination of p-cresol concentrations in hydrolysate samples was performed using the calibration curve for p-cresol and is provided in Table 2.

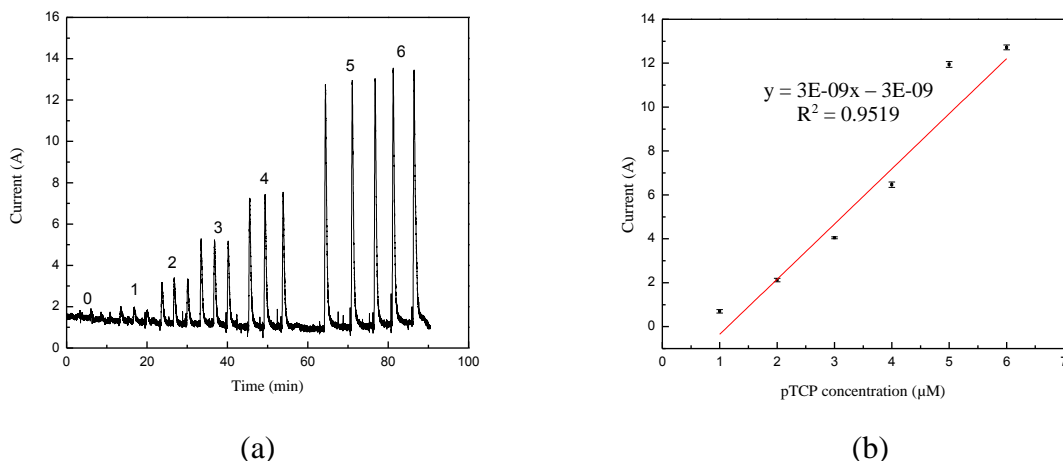


Figure 14: (a) Amperometry of products of pTCP alkaline hydrolysis reaction enhanced by ultrasonic irradiation. Initial concentrations of pTCP (μM) before the reaction are shown as numbers over the peaks. (b) Linear plot of amperometry of the products of pTCP alkaline hydrolysis enhanced by ultrasonic irradiation. Data points correspond to the 3 repetitions of amperometry. Error bars are the standard deviation of the 3 repetitions. Note: current of $0 \mu\text{M}$ pTCP injections was subtracted from all sample peak currents. The R^2 coefficient of the linear fit is 0.9519.

Table 2: Determination of p-cresol concentration in product of alkaline hydrolysis of pTCP enhanced by ultrasonic irradiation using the p-cresol calibration curve (Figure 12).

Amperometric current, nA	Initial pTCP concentration, nM	P-cresol concentration in product of hydrolysis of pTCP, nM
0.699 ± 0.08	1000	320
2.12 ± 0.08	2000	604
4.05 ± 0.05	3000	990
6.46 ± 0.12	4000	1472
11.9 ± 0.13	5000	2560
12.7 ± 0.11	6000	2720

4.5 Spectrophotometric Detection of Product of Ultrasonic Irradiation -

Enhanced pTCP Hydrolysis

UV-vis absorption spectra measurements of product of ultrasonic irradiation-enhanced alkaline hydrolysis show an absorbance peak between 510 and 530 nm which corresponds to the p-cresol peak (Figure 15). The samples with concentrations ranging from 10 to 100 μM (pTCP) were analyzed. The arrow on Figure 15 indicates the direction of the initial pTCP concentrations decrease. The red line on the spectra with the highest absorbance corresponds to the 100 μM initial pTCP concentration. Lower concentrations of pTCP did not show absorbance peaks, thus limit of detection, in terms of the initial pTCP concentration at the reaction inception, is 100 μM . Using the calibration curve of UV-Vis absorption spectra of p-cresol (Figure 13b), it is possible to see that the red line corresponds to, approximately, 87.8 μM p-cresol. Overall, UV-vis spectrophotometry has a lower sensitivity compared to amperometry.

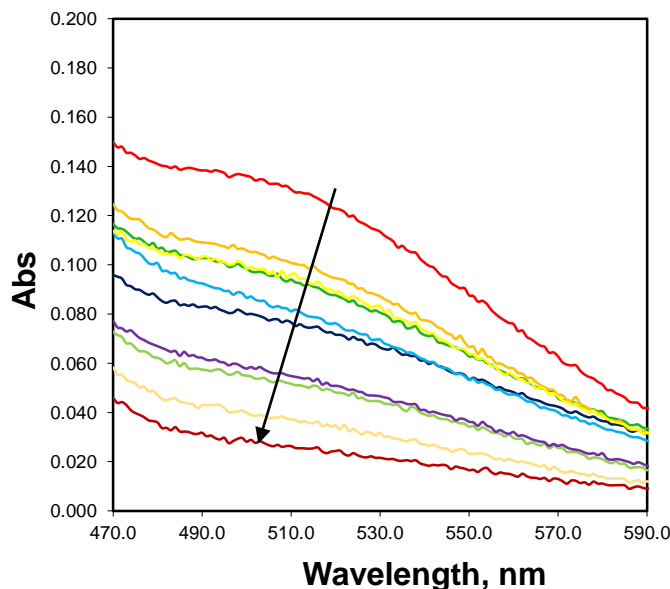


Figure 15: UV-Vis absorption spectra of product of ultrasonic irradiation-enhanced pTCP hydrolysis. Samples of concentration range from 10 to 100 μM in terms of initial

pTCP concentration were analyzed. The arrow indicates the direction of the pTCP concentrations decrease. The absorbance peak is observed between 510 and 530 nm, which allows to detect the product of hydrolysis, cresol. Limit of detection is 100 μM pTCP.

4.6 Boiling - Enhanced pTCP Hydrolysis. Electrochemical Detection of Product

Amperometry of the product of boiling-enhanced pTCP hydrolysis was performed in a flow mode. Concentrations ranging from 1000 nM to 6000 nM in terms of initial pTCP concentrations were utilized for detection of cresol. Figure 16 shows the quantitative results of the amperometric detection of the product. Table 3 provides the information on p-cresol concentrations in the tested product of hydrolysis. Determination of p-cresol concentrations was performed using the amperometric calibration curve for p-cresol (Figure 12).

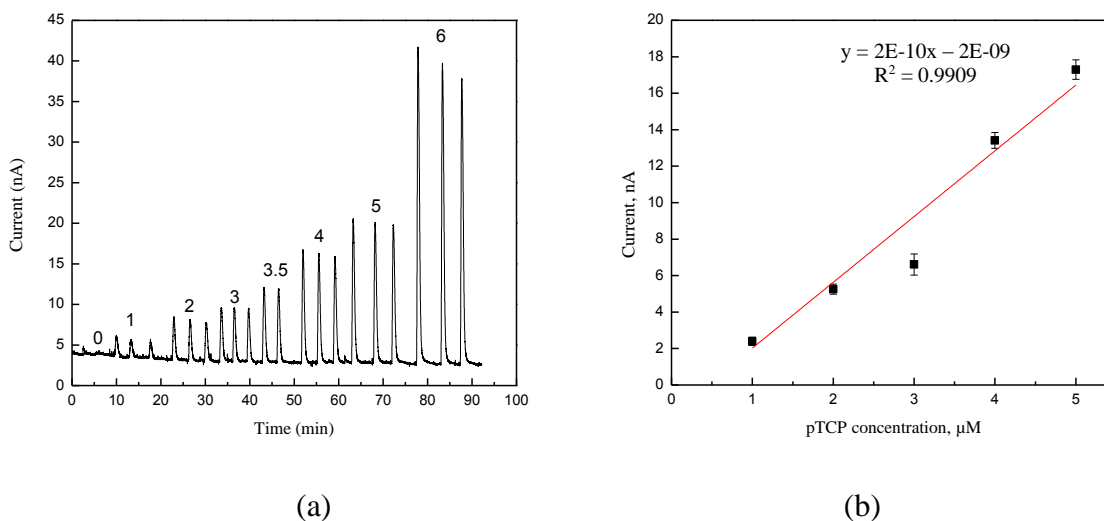


Figure 16: (a) Amperometry of products of pTCP alkaline hydrolysis reaction enhanced by boiling. Initial concentrations of pTCP (μM) before the reaction are shown as

numbers over the peaks. Each sample was injected 3 times and generated 3 peaks, with the exception of 3.5 μM pTCP sample. (b) Linear plot of amperometry of the products of pTCP alkaline hydrolysis enhanced by boiling. Data points correspond to the 3 repetitions of amperometry. Error bars are the standard deviation of the 3 repetitions. Note: current of 0 μM pTCP injections was subtracted from all sample peak currents. The 6 μM pTCP sample was not used in this plot. The R^2 coefficient of the linear fit is 0.9909.

Table 3: Determination of p-cresol concentration in product of alkaline hydrolysis of pTCP enhanced by boiling using the p-cresol amperometric calibration curve (Figure 11).

Amperometric current, nA	Initial pTCP concentration, nM	P-cresol concentration in product of hydrolysis of pTCP, nM
2.40 \pm 0.23	1000	659.3
5.26 \pm 0.27	2000	1231.3
6.61 \pm 0.58	3000	1501.4
13.40 \pm 0.43	4000	2862.9
17.30 \pm 0.54	5000	3639.5
36.91 \pm 1.6	6000	7562.9

4.7 Spectrophotometric Detection of Product of Boiling - Enhanced pTCP

Hydrolysis

Product of boiling-enhanced pTCP hydrolysis was tested via UV-vis spectrophotometry for validation of the cresols production (Figure 17). An absorbance peak between 510 and 530 nm was observed, which corresponds to p-cresol.

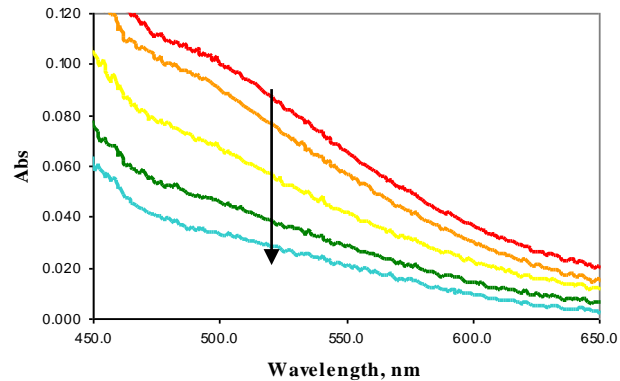


Figure 17: UV-Vis absorption spectra of product of boiling-enhanced pTCP hydrolysis. Samples of concentration range from 60 to 100 μM in terms of initial pTCP concentration are shown. The arrow indicates the direction of the pTCP concentrations decrease. The absorbance peak is observed between 510 and 530 nm, which allows to detect the product of hydrolysis, cresol. Limit of detection is 100 μM pTCP.

The red line on the spectra corresponds to the 100 μM initial pTCP concentration. As in the case of product of ultrasonic irradiation-enhanced hydrolysis, lower concentrations of pTCP did not show absorbance peaks. In terms of the initial pTCP concentration in the reaction mixture at the reaction inception, limit of detection is 100 μM . The red line on Figure 17, which corresponds to, approximately, 93.8 μM p-cresol, represents the limit of detection. Calibration curve of UV-Vis absorption spectra of p-cresol (Figure 12b) allowed to make this conclusion.

Chapter 5. Overall Conclusions and Suggestions for Future Work

Rapid detection of TCP on board the aircraft is a challenging task. This thesis discusses a novel approach to acceleration the hydrolysis of pTCP and a use of electrochemical techniques to detect the electroactive product of hydrolysis. This work serves as the basis for implementation of a sensing device capable of detecting pTCP on board an aircraft. Electrochemical detection approach is a highly sensitive technique which has a potential for application in portable sensors due to its high sensitivity, scalability, time and cost-effectiveness. Ultrasonic irradiation is an effective and safe method for enhancing the hydrolysis of organophosphates. Other studies of hydrolysis reaction rely on the heat treatment (230 °C) of TCP solution in an oil bath for reaction enhancement, followed by TCP vaporization and hydrolysis reaction of gaseous TCP with solid NaOH on Al₂O₃ carrier [35]. Compared to ultrasonic irradiation set-up described in this thesis, scalability limitations of the heat treatment and evaporation set-up [35] exist. Amperometric detection limit of p-cresol was demonstrated in this thesis as 500 nM, with signal-to-noise ratio (S/N=3), which shows an improvement compared to the electrochemical detection limit of 600 nM reported previously [60]. A consequence of combining ultrasonic irradiation and electrochemical detection have yielded a system that detects pTCP, meaning a portable and usable by aircrew sensor may be realized with further work and implementation. Studies show that airborne pTCP levels in an event of an air supply contamination on an aircraft are between 0.5 µg/m³ (0.031 ppb) and 49

$\mu\text{g}/\text{m}^3$ (3.02 ppb) [17]. According to the previous reports on pTCP concentration conversion from molarity to ppb in air, the range of 0.5 to 100 μM in solution corresponds to the range of 0.5 to 100 ppb in air [34]. Taking into account this conversion approach, the results of electrochemical detection are applicable to the studies of the contamination of cabin air by pTCP.

This work has also demonstrated a higher sensitivity of amperometric detection compared to spectrophotometric approach. Amperometry demonstrated the limit of detection of pure p-cresol as 500 nM, in contrast, spectrophotometry limit of detection was 100 μM . UV-Vis spectrophotometry was used as a validation technique for detection of products of pTCP hydrolysis, and is not recommended as a primary technique.

Future work could focus on using ultrasonic irradiation and electrochemical techniques for testing the detection of TCP in jet engine oils. Optimization of catalysis of hydrolysis also has yet to be realized in this work. Working electrode surface modification could also be studied for prospects of improving the sensitivity and reusability by minimizing the electrode fouling phenomenon. Application of enzymes in the design of electrochemical sensor would be another promising direction of future work that could significantly improve the sensitivity of a sensor. Organophosphorus hydrolase could be employed as a catalyst for hydrolysis process. Multi-analyte detection approach for discriminative detection of TCP could be investigated.

This work is only the initial part of developing an onboard detection system for TCP, as further optimization steps could be performed. Miniaturization of a sensor may be required for potential application on board the aircraft.

References

1. Eggins BR (2002) *Chemical Sensors and Biosensors*. Wiley & Sons Inc.
2. Diamond D (1998) *Principles of Chemical and Biological Sensors*. Wiley & Sons Inc.
3. Wang J (2000) *Analytical Electrochemistry: 2nd ed.* Wiley & Sons Inc.
4. Vetelino J, Reghu A (2011) *Introduction to Sensors*. CRC Press, New York.
5. Mohammed AA (2013) *Electrochemistry*. InTech.
6. Dunn PF (2011) *Fundamentals of Sensors for Engineering and Science*. CRC Press.
7. Michael AC, Borland LM (2007) *Electrochemical Methods for Neuroscience*. CRC Press, Taylor & Francis.
8. Heitcamp MA, Huckins JN, Petty JD, Johnson JL (1984) Fate and metabolism of isopropylphenyl diphenyl phosphate in fresh-water sediments. *Environ. Sci. Technol.* 18: 434 - 439.
9. Montgomery MR, Wier GT, Zieve FJ, Anders MW (1977) Human intoxication following inhalation exposure to synthetic jet lubricating oil. *Clin Toxicol* 11: 423–6.
10. Murawski JTL, Supplee DS (2008) An attempt to characterize the frequency health impact, and operational costs of oil in the cabin and flight deck supply air on U. S. Commercial Aircraft. *J ASTM Int* 5: 1–15.
11. Ross SM (2008) Cognitive function following exposure to contaminated air on commercial aircraft: a case series of 27 pilots seen for clinical purposes. *J Nutr Environ Med* 17:111–26.

12. Van Netten C, Leung V (2001) Hydraulic fluids and jet engine oil: pyrolysis and aircraft air quality. *Arch Environ Health* 56:181–6.
13. Winder C (2006) Hazardous chemicals on jet aircraft: case study – jet engine oils and aerotoxic syndrome. *Curr Top Toxicol* 3:65–88.
14. Winder C, Michaelis S (2005) Aircraft air quality malfunction incidents – crew effects from toxic exposures on aircraft. *Air quality in airplane cabins and similar enclosed spaces. The handbook of environmental chemistry, vol. 4. Heidelberg: Springer-Verlag; p. 211–28 Part H.*
15. Zhang T, Chen Q (2007) Novel air distribution systems for commercial aircraft cabins. *Building and Environment* 42: 1675–1684.
16. Wu C, Ahmed NA (2012) A novel mode of air supply for aircraft cabin ventilation. *Building and Environment* 56: 47-56.
17. National Research Council (2002) *The airliner cabin environment and the health of passengers and crew.* National Academy Press, Washington, DC.
18. Hale MA, Al-Seffar JA (2009) Preliminary report on aerotoxic syndrome (AS) and the need for diagnostic neurophysiological tests. *Am J Electroneurodiagnostic Technol* 49: 260-79.
19. Winder C, Balouet JC (2002) The toxicity of commercial jet oils. *Environ Res* 89:146-64.
20. Bernabei M, Secli R, Bocchinfuso G (2000) *Microcolumn Sep.* 12: 585.
21. Kibby J, DeNola G, Hanhela PJ, Mazurek W (2005) *Defence Science and Technology Organisation, Department of Defence, DSTO-RR-0292, Melbourne.*

22. Kinugasa H, Yamaguchi Y, Miyazaki N, Okumara M, Yamamoto Y, et al. (2001) 67, 696.
23. Casida JE, Gammon DW, Glickman AH, Lawrence LJ (1983) *Ann Rev Pharmacol Toxicol* 23: 413.
24. Abou-Donia MB, Lapadula DM (1990) *Ann. Rev. Pharmacol. Toxicol.* 30: 405.
25. Hatch RC (1988) Poisons causing nervous stimulation or depression. In N.H. Booth and L.E. McDonald (Eds.), *Veterinary Pharmacology and Therapeutics*, Iowa State University Press, Ames, IA, p. 1053 (1988).
26. Rosenstock L et al. (1991) Chronic central nervous system effects of acute organophosphate pesticide intoxication. *Lancet* 338 (8761): 223-227.
27. Craig PH, Barth ML (1999) *J. of toxicology and environmental health-part B-critical reviews* 2, 281.
28. Habboush AE, Farroha SM, Khalaf HI (1995) Extraction-gas chromatographic method for the determination of organophosphorus compounds as lubricating oil additives. *Journal of Chromatography A* 696: 257–263.
29. Ofstad EB, Sletten T (1985) Composition and water solubility determination of a commercial tricresylphosphate. *Science of the Total Environment* 43: 233–241.
30. Mutsuga M, Kawamura Y, Watanabe Y, Maitani T (2003), Determination method of tricresyl phosphate in polyvinyl chloride. *Food Hygiene and Safety Science* 44: 26–31.
31. Bhattacharyya J, Bhattacharyya K, Sengupta PK, Ganguly SK (1974) Detection and estimation of tricresyl phosphate in mustard oil. *Forensic Science* 3: 263–270.
32. Barsoum BN, Watson WM, Mahdi IM, Khalid E (2004) Electrometric assay for the determination of acetylcholine using a sensitive sensor based on carbon paste. *J.*

Electroanal. Chem. 567: 277–281.

33. De Nola G, Kibby J, Mazurek W (2008) Determination of ortho-cresyl phosphate isomers of tricresyl phosphate used in aircraft turbine engine oils by gas chromatography and mass spectrometry. *J. Chromatogr. A* 1200: 211–216.
34. Yang X, Zitova A, Kirsch J, Fergus JW, Overfelt RA, Simonian AL (2012) Portable and remote electrochemical sensing system for detection of tricresyl phosphate in gas phase. *Sensors and Actuators B* 161: 564 – 569.
35. Yang X, Kirsch J, Olsen EV, Fergus JW, Simonian AL (2013) Anti-fouling PEDOT:PSS modification on glassy carbon electrodes for continuous monitoring of tricresyl phosphate. *Sensors and Actuators B* 177: 659 – 667.
36. Yang X, Kirsch J, Zhang Y, Fergus JW, Simonian AL (2013) Potential Drop Based Model to Analyze Electrode Passivation by Fouling from Phenolic Compounds. *ECS Transactions* 53 (35): 1 - 14.
37. Belskii VE (1977) Kinetics of the Hydrolysis of Phosphate Esters. *Russian Chemical Reviews* 46 (9): 1578 – 1603.
38. Vajnhandl S, Marechal AML (2005) Ultrasound in textile dyeing and the decolourization/mineralization of textile dyes. *Dyes Pigments* 65: 89–101
39. Suslick KS (1989) The Chemical Effects of Ultrasound. *Sci. Am.*: 260: 80–6.
40. Collins E (1945) Reaction of Diazotised P-nitraniline with Phenols: Detection of Tricresyl Phosphate in Edible Oil. *Analyst* 70: 326-330
41. Luche JL (1998) *Synthetic Organic Sonochemistry*. Plenum Press: New York.
42. Lorimer J, Mason T (1987) *Sonochemistry Part 1 - The Physical Aspects*. *Chem. Soc. Rev.* 16: 239.

43. Young FR (1989) Cavitation. McGraw-Hill: New York.
44. Flint EB, Suslick KS (1991) The Temperature of Cavitation. *Science* 253: 1397.
45. Suslick K (1990) Sonochemistry. *Science* 247: 1439.
46. Adewuyi YG (2001) Sonochemistry: Environmental Science and Engineering Applications. *Ind. Eng. Chem. Res.* 40: 4681-4715.
47. Destailats H, Hoffmann MR, Wallace HC (2003) Sonochemical degradation of pollutants. In: Tarr MA (ed) *Chemical degradation methods for wastes and pollutants. Environmental and industrial applications.* Marcel Dekker, Inc., USA
48. Chen D (2012) Applications of ultrasound in water and wastewater treatment. In: Chen D, Sharma SK, Mudhoo A (eds) *Handbook on application of ultrasound: sonochemistry for sustainability.* CRC Press, Taylor & Francis Group, Boca Raton
49. Yasuda K, Koda S (2012) Development of sonochemical reactor. In: Chen D, Sharma SK, Mudhoo A (eds) *Handbook on application of ultrasound: sonochemistry for sustainability.* CRC Press, Taylor & Francis Group, Boca Raton
50. Macalady DL, Wolfe NL (1985) Effect of sediment sorption and abiotic hydrolyses. 1. Organophosphorothioate esters. *J. Agric. Food Chem.* 33: 167-173.
51. How it works. Available: <http://www.howitworksdaily.com/how-do-cabin-air-systems-work/>
52. Vertelov GK, Gale FW, Simonian AL (2006) TCP Electrochemical Detection. *ECS Transactions*: 3 (10) 21 – 34.
53. Muir DCG, Yarechewski AL, Grift NP (1983) Environmental dynamics of phosphate esters. III. Comparison of the bioconcentration of four triaryl phosphates by fish. *Chemosphere* 12 (2): 155 – 166.

54. LeBel GL, Williams DT (1983) Determination of organic phosphate triesters in human adipose tissue J Assoc Off Anal Chem 66(3): 691 – 699.
55. Nomeir AA, Abou-Donia MB (1983) High-performance liquid chromatographic analysis on radial compression column of the neurotoxic tri-*o*-cresyl phosphate and metabolites. Analytical Biochemistry: 135 (2) 296 – 303.
56. Chakrabarty MM, Bandyopadhyay C, Bhattacharyya D, Gayen AK (1968) Detection of adulteration of fats by thin layer chromatography of trisaturated glycerides : I. Detection of hydrogenated groundnut oil, tallow and Mohua (Mowrah) oil in butter fat (ghee). J. Chromatog. 36: 84 – 90.
57. Ishikawa S, Taketomi M, Shinohara R (1985) Determination of trialkyl and triaryl phosphates in environmental samples. Water Research 19 (1): 119-125.
58. Chang JL, Thompson JE (2010) Characterization of colored products formed during irradiation of aqueous solutions containing H₂O₂ and phenolic compounds. Atmospheric environment 44: 541-551.
59. Chowdhury P, Viraraghavan T (2009) Sonochemical degradation of chlorinated organic compounds, phenolic compounds and organic dyes – A review. Sci. of the total Envir. 407 (8): 2474-2492.
60. Pedrosa VA (2009) Copper nanoparticles and carbon nanotubes-based electrochemical sensing system for fast identification of tricresyl phosphate in aqueous samples and air. Sensors and Actuators B: Chemical 140 (1): 92-97.